

JOURNAL OF ADVANCED APPLIED SCIENCES

e-ISSN: 2979-9759



RESEARCH ARTICLE

Frequency Dependent Negative Dielectric Behavior in Parylene C Based Composite Films

Utku Guduloglu¹ • Sedat Kurnaz² • Turgay Seydioglu³ • Gizem Bekar⁴ • Ozgur Ozturk⁵ •

ARTICLE INFO

Article History

Received: 22.04.2024 Accepted: 04.06.2024 First Published: 22.06.2024

Keywords

Dielectric Negative capacitance Parylene C Polymer



ABSTRACT

Dielectric materials are an important research topic for many applications today. Polymers are among the prominent dielectrics due to their durability, high ionic conductivity and low dielectric losses. This study investigates the dielectric properties of Parylene C (PAC)-based composite films. Capacitance and dissipation factor values are measured. Dielectric permittivity and losses are calculated. Negative capacitance and negative dielectric constant are observed, and resonant frequency values are compared. Activated carbon doping significantly impacts the resonant frequencies of the films. Doped samples exhibit higher positive and negative resonant frequencies (2.2560 MHz and 2.2593 MHz) compared to undoped counterparts (2.1952 MHz and 2.2015 MHz). Polarization further increases resonant frequencies, alongside dielectric permittivity and dissipation factor with permittivity experiencing a more pronounced increase. Post-polarization, doped samples display resonant frequencies of 2.3727 MHz and 2.3761 MHz, while undoped samples reach 2.3658 MHz and 2.3727 MHz. A comprehensive analysis of impedance, resistance, and reactance values reveals insights into the composite film's behavior. Crucially, throughout the measurements, the composite films display a consistent inductive response at frequencies above their resonance frequencies. Understanding the mechanisms behind this inductive response could open up new possibilities for the use of these films in advanced electronic devices and circuits.

Please cite this paper as follows:

Guduloglu, U., Kurnaz, S., Seydioglu, T., Bekar, G., & Ozturk, O. (2024). Frequency dependent negative dielectric behavior in parylene C based composite films. *Journal of Advanced Applied Sciences*, *3*(1), 32-39. https://doi.org/10.61326/jaasci.v3i1.254

1. Introduction

Negative capacitance effect in ferroelectric materials has attracted many researchers' attention recently (Wong & Salahuddin, 2018). The presence of negative capacitance in a material means that the material exhibits an inductive behaviour (Jones et al., 1998). The Landau-Ginzburg-Devonshire model,

which models the phenomena in ferroelectric materials, explains the emergence of the definition of negative capacitance. According to this model, in the energy barrier region between energy minima, where the polarisation value is close to 0 ($P\approx0$), the ferroelectric has negative capacitance (Hoffmann et al., 2019). Another explanation for the negative

E-mail address: sedatkurnaz@kastamonu.edu.tr



32

¹Bartın University, Faculty of Engineering, Architecture and Design, Department of Electrical and Electronics Engineering, Bartın/Türkiye

²Kastamonu University, Central Research Laboratory, Kastamonu/Türkiye

³Kastamonu University, Vocational School, Department of Electronics and Automation, Kastamonu/Türkiye

⁴Sinop University, Ayancık Vocational School, Department of Electronics and Automation, Sinop/Türkiye

⁵Kastamonu University, Faculty of Engineering and Architecture, Department of Electrical and Electronics Engineering, Kastamonu/Türkiye

[™] Correspondence

capacity is the reduction of the effective voltage across the capacitor during ferroelectric switching. Examples of potential applications of negative capacitance materials today include field-effect transistors, energy storage, high-power microwave filters (Hoffmann et al., 2019; Sun et al., 2019). Negative capacitance has been difficult to measure because the material does not exhibit stable behaviour in the negative capacitance state. However, since materials with negative capacitance behaviour show the characteristics of a series inductorcapacitor circuit, stabilisation can also be achieved in the negative capacitance state by using the series capacitor model (Khan et al., 2015; Z. Wang et al., 2020). In the series capacitor model, the total capacitance is equal to the series equivalent of the capacitance of each dielectric, and "dielectric resonance" occurs when the frequency takes on the value $f=1/2\pi(LC)$, thus clearly obtaining negative capacitance in the resonant frequency region. In the negative capacitance state, the capacitor spontaneously charges. This saves energy by enabling nanoelectronic applications with very low power consumption (Íñiguez et al., 2019).

The dielectric constant (ε_r) also known as relative permittivity, is a fundamental material property that quantifies the ability of a substance to store electrical energy within an electric field. It serves as a critical parameter in diverse fields such as materials science, chemistry, and physics. The dielectric constant significantly influences the polarization behavior, energy storage capacity, and overall electrical properties of materials. The real component of the dielectric constant is represented by dielectric permittivity (ε), while the imaginary component is represented by dielectric loss (ε'') (Xie et al., 2022). Materials exhibiting negative capacitance necessarily possess negative permittivity due to the relationship described by the equation: $C = \varepsilon_0 \varepsilon_r A/d$ where ε_0 is the vacuum permittivity, ε_r is the dielectric permittivity, A is the surface area of the sample and d is the thickness of the film. Negative permeability is a phenomenon typically observed at frequencies of megahertz (MHz) and above (Yan et al., 2013). The Drude and Lorentz models are instrumental in elucidating the behavior of negative permittivity, not negative permeability. The Drude model, a cornerstone in understanding the transport properties of electrons in metals, describes electron conduction in solids by considering induced electronic polarization. This is achieved by introducing an auxiliary particle, attached to each polarizable atom via a harmonic spring (Jiang et al., 2010). According to the Drude model, when the contribution of the conducting material surpasses a certain threshold, the structure becomes conductive, and the collective movement of electrons results in negative permittivity.

The Lorentz resonance model is a fundamental concept used to understand the behavior of resonant systems, particularly in the context of electromagnetic phenomena. This model finds widespread application in fields like optics, materials science, and physics to analyze and predict the response of resonant systems to external stimuli (Oughstun & Cartwright, 2003; Romano et al., 2014). According to the Lorentz model, when the doping concentration of a conducting material is below the percolation threshold, the conducting phase remains isolated, and induced dipoles form. These dipoles, through resonance, can cause the dielectric constant to decrease, potentially reaching negative values. However, it is important to note that both the Drude and Lorentz models have limitations in fully explaining the complexities of dielectric behavior (Leng et al., 2020). A negative dielectric constant signifies a situation where charges align in the opposite direction to the applied voltage. In recent years, there has been growing interest in metamaterials exhibiting this property. Potential applications of metamaterials with negative dielectric constants include sensors, antennas, wireless transmission systems, and capacitors (Qu et al., 2019; Balu et al., 2020; Liu et al., 2020).

Complex impedance spectroscopy is an important study commonly used for observe the dielectric properties of dielectric materials. Impedance is a complex parameter that indicates the resistance of a material to alternating current and can be expressed by the expression Z = R + jX or Z = Z' + jZ''. Here R is the resistance, which is the real part of the impedance, and X is the reactance, which is the imaginary part of the impedance (El-Nahass et al., 2014; Sankar et al., 2022). Impedance analyses has been used to characterize some materials including polymers and developed some electronic devices (Raja et al., 2004).

Polymer dielectrics are commonly used in various applications due to their lightweight nature, scalability, mechanical flexibility, high dielectric strength, and reliability. However, these materials face limitations, particularly in high temperature (exceeding 150 °C) and high energy storage applications. Furthermore, the dielectric constants of polymer materials are often limited and it is not meet the requirements for high energy storage dielectric capacitors (Dong et al., 2023). Also, the flashover issue at the interfaces of polymer dielectrics with other substances poses a significant challenge, as the breakdown voltages at these interfaces are lower than those for the dielectrics alone, affecting the safe and reliable operation of the materials (T. Wang et al., 2022). So, to remove these limitations, the development of polymer nanocomposites with rationally designed nanostructured inorganic fillers has shown promise in improving the capacitive performance of polymer materials (Li et al., 2019).

In this study, we investigate the dielectric properties of PAC-based composite films, focusing on the influence of activated carbon doping. The analysis encompasses the impact of doping on resonant frequency, negative capacitance regions, dielectric permittivity and losses, and complex impedance parameters. Furthermore, we examine the effects of the polarization process on the dielectric properties of the composite films.

2. Materials and Methods

The synthesis process of PAC consists of three steps: sublimation, pyrolysis, and deposition. In the sublimation step, the granular dimer was vaporized at 150 °C. The dimeric gas was transferred to the pyrolysis furnace using argon gas and a vacuum pump. In the pyrolysis step, the dimeric gas was then split into a monomeric gas at a temperature of 650 °C. Finally, the monomeric gas was released into the coating chamber to be deposited on the glass substrate under a vacuum of 0.6 Pa at room temperature. To capture the excess PAC, a cold trap was placed in front of the pumping system. After deposition, the PAC films were removed from the glass substrate by using a tweezers and acetone. The synthesized PAC was dissolved in 50 ml of 1, 2 dichlorobenzene at 160 °C for 6 h with stirring. The PU, PMMA, and AC were added in different weight ratios to mix the solution homogeneously for 1 h at the same temperature. The solution was cooled by mixing, and 20 ml of acetone at 50 °C was added and stirred for 30 min. The samples were labelled as 0C and 1C based on the weight ratio of the ACs in the polymer matrix (Table 1) (Kurnaz et al., 2023).

Table 1. The mass ratio of polymer composites in the mixture.

Samples	PAC (%)	PU (%)	PMMA (%)	AC (%)
0C	50	45	5	0
1C	50	44	5	1

Capacitance measurements were carried out by an impedance analyzer (Wayne Kerr 6500B) at 1-10 MHz with a 1 $V_{\rm AC}$ signal at room temperature. At the same time, the dielectric properties were examined with an impedance analyser as a result of polarisation processes by applying 1 kV voltage for 10 minutes at 60 °C temperature.

3. Results and Discussion

Figure 1a shows the frequency dependence of the capacitance value of the samples prior to polarisation. The graph clearly shows the resonance frequency value and the peaks that occur in this region. It can be seen that the activated carbon additive causes a shift in the resonance frequency region. For 0C, the positive resonant frequency is 2.1952 MHz and the negative resonant frequency is 2.2015 MHz. For the 1C, the positive and negative resonant frequencies are 2.2560 MHz and 2.2593 MHz respectively. The transition to negative capacitance is clearly seen at frequencies after the positive resonant frequency. This shows that the inductive behaviour dominates the capacitive behaviour from the positive resonant frequency of the film. The resonance frequencies of 1C are higher than those of OC. They are shifted towards higher frequencies. In the measurements made after polarisation, the resonant frequencies are slightly higher than before polarisation (Figure 1b). It can be seen that this also leads to an increase in the values of the capacitance. For the 0C, the positive resonant

frequency is 2.3658 MHz and the negative resonant frequency is 2.3727 MHz. For 1C the positive and negative resonant frequencies are 2.3727 MHz and 2.3761 MHz respectively. Depending on the polarisation, the change at 1C is greater than 1.8 pF and the change at 0C is 11.91 pF. This is actually due to the decrease in the amount of PU in the film, which exhibits dielectric behaviour (Vandeparre et al., 2013; D. Wang et al., 2013). The frequency dependence of the permittivity of the samples before and after polarisation is shown in Figure 1c and 1d. The value of the dielectric constant is calculated from capacitance measurements. The permittivity is directly proportional to the capacitance and shows a similar behaviour to Figure 1a and 1b. The permittivity at the positive resonant frequency is 44.23 for the 0C and 77.01 for the 1C. It is -72.85 for 0C and -25.34 for 1C at the negative peak resonant frequency (Figure 1c).

After polarisation, the permittivity at the positive resonant frequency is 246.6 for 0C and 58.58 for 1C. At the negative peak resonant frequency, it is calculated to be -31.25 for 0C and -25.34 for 1C. It can be seen that polarisation reduces the negative permittivity values (Figure 1d). Mokni et al. (2019) measured the dielectric permittivity value of PAC to be approximately 5 at a frequency of 1 MHz. In other studies, results are obtained that show a low dielectric permittivity (Kahouli et al., 2009; Hu et al., 2022). In this study, it is quite high in the PAC-based composite film. At a frequency of 1 MHz, the dielectric constant before polarisation is 23.46 for the 0C sample and 23.72 for the 1C sample, while it is measured to be 26.68 for the 0C sample and 25.54 for the 1C sample after polarisation. The resonance behavior of permittivity can be explained with Lorentz model. According to Lorentz model, the permittivity is;

$$\varepsilon_r = 1 + \frac{\omega_p^2 (\omega_0^2 - \omega^2)}{(\omega_0^2 - \omega^2)^2 + \omega \omega_r^2} \tag{1}$$

where $\omega_0 = 2\pi f_0$ is the characteristic frequency, ω is angular frequency, ω_{τ} is a damping frequency, and ω_p is the transverse frequency of lattice vibration. We can see in model and the figures, when ω is less than ω_0 , permittivity is negative and samples show the inductive character (Z. Wang et al., 2020). The resonance behavior is observed because of the piezoelectric resonance effect of PAC (Yang et al., 2022).

Figure 1e and 1f shows the frequency dependent variation of the dielectric loss value of the samples before and after polarisation. We observed that negative dielectric loss values for the bigger frequency values than the resonance frequency. Negative dielectric loss means that the energy released is more than the energy absorbed (Axelrod et al., 2006). The peak values of dielectric loss at positive and negative resonance frequencies before polarisation are 459.6761 and -7552.6788 for 0C, and 4195.3025 and -244.2922 for 1C respectively, and after polarisation 2368.0796 and -191.2578 for 0C and 554.1878 and -883.5565 for 1C respectively.

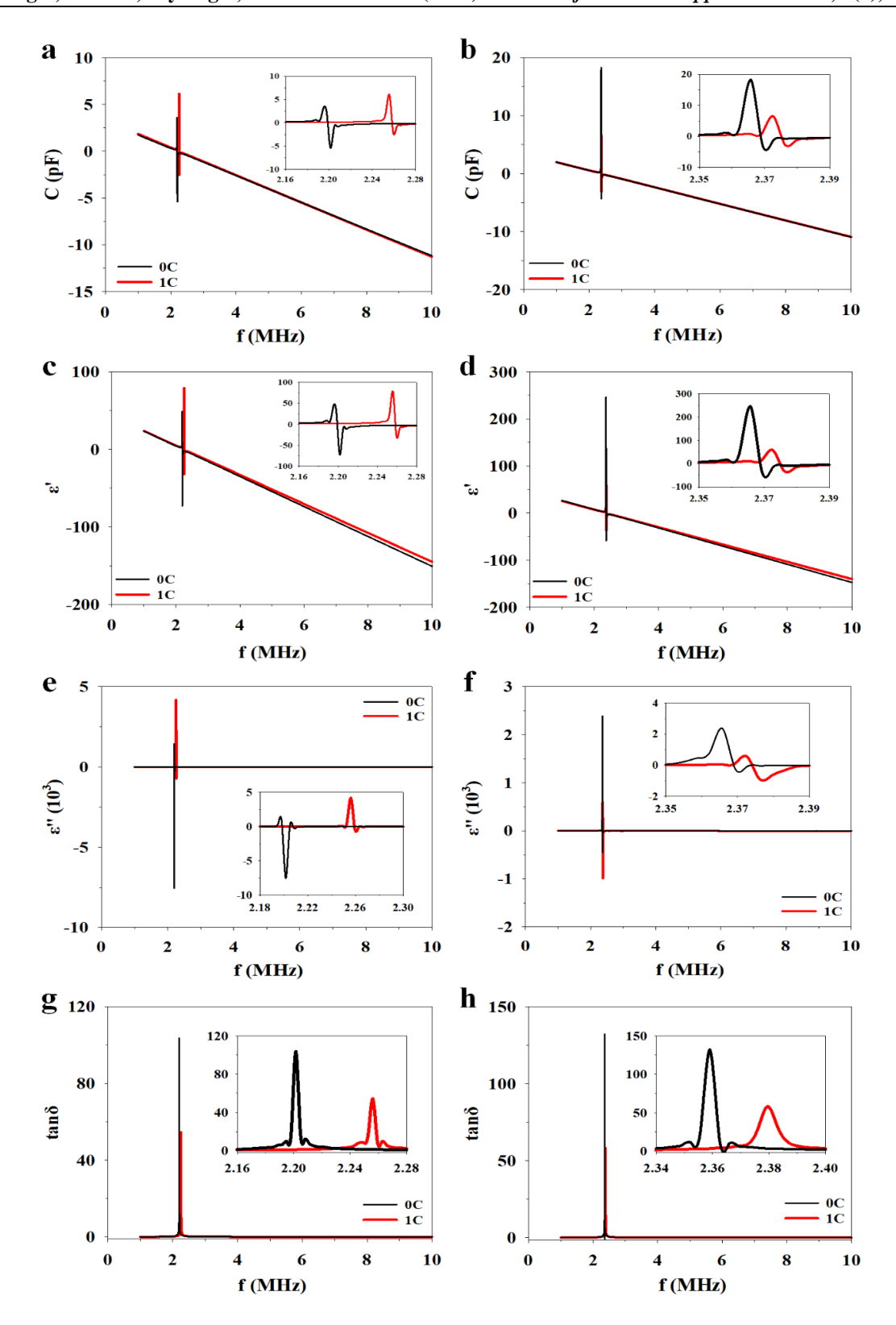


Figure 1. Frequency-dependent (a) capacitance, (c) permittivity, (e) dielectric loss, (g) dissipation factor before polarisation and (b) capacitance, (d) permittivity, (f) dielectric loss, (h) dissipation factor after polarisation measurements of 0C and 1C samples.

Figure 1g and 1h shows the frequency dependent variation of the dissipation factor value of the samples before and after polarisation. The dissipation factor is a parameter that indicates the amount of energy lost at a given frequency value

(Florkowski et al., 2024). It is equal to the ratio of the imaginary part of the dielectric permittivity to the real part $(tan\delta = \varepsilon''/\varepsilon')$. It can be seen that the dissipation factor reaches the highest values in the resonance frequency regions. 103.67 for 0C and

54.47 for 1C. The dissipation factor of 0C is higher than that of 1C (Figure 1g). After polarisation, the dissipation factor increases to 132.2 for 0C and 58.19 for 1C (Figure 1h). These values indicate that although polarisation increases the loss factor, this increase is much less than the rate of increase in permittivity and therefore it can be said that polarisation contributes positively to the permittivity of the film. It is noted that dissipation factor values of less than 5% are generally accepted as low dielectric loss (Z. Wang et al., 2020). The dissipation factor values outside the resonant frequency range

are very low in the measured frequency range. In general, there are polymers with very low loss values, but losses at 1 MHz frequency are up to 0.09 (Yu et al., 2008; Xu et al., 2013). In our study, this value is 0.0271 for the 0C before polarisation, 0.0197 for the 1C, 0.0266 for the 0C sample after polarisation and 0.0224 for the 1C sample. In the resonant frequency region, a high permeability frequency range can be obtained where the dielectric constant is negative and the dissipation factor is low. The characteristic situation in this region is very suitable for the realisation of metamaterial applications (Z. Wang et al., 2020).

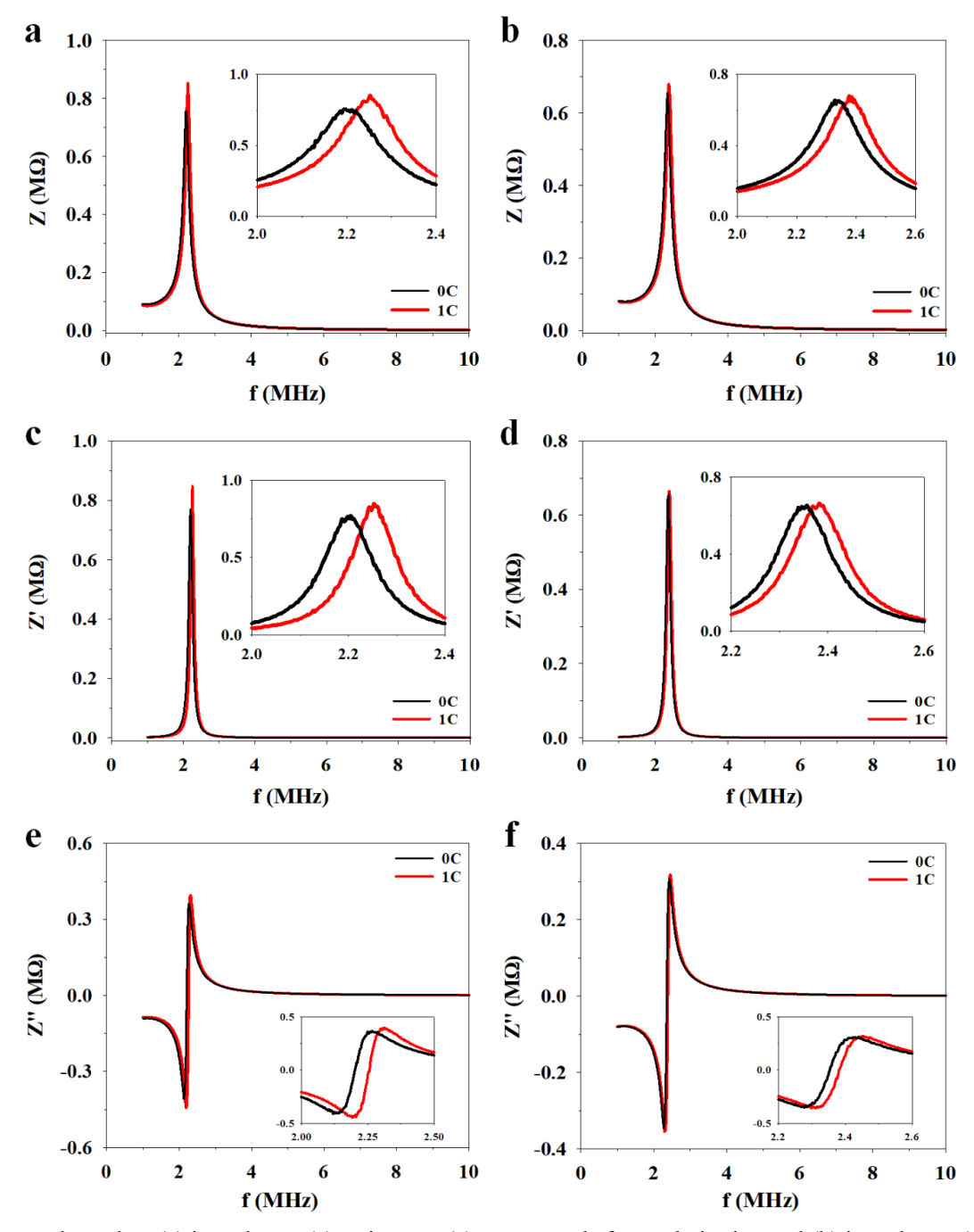


Figure 2. Frequency-dependent (a) impedance, (c) resistance, (e) reactance, before polarisation and (b) impedance, (d) resistance, (f) reactance, after polarisation measurements of 0C and 1C samples.

Figure 2a shows the frequency variation of the impedance value of the samples before and after polarisation. At the resonance frequency, the impedance value takes the peak. The peak values are 0.7533 M Ω for the 0C and 0.8527 M Ω for the 1C before polarisation (Figure 2a). The impedance values after polarisation in Figure 2b are $0.6375 \text{ M}\Omega$ for the 0C and 0.6797 $M\Omega$ for the 1C. A decrease in impedance values after polarisation is observed, and when the active carbon added, the peak of impedance value increased. While it is generally understood that active carbon enhances electrical conductivity and charge transfer capabilities, the specific interactions within the composite material, such as the distribution of active carbon within the polymer matrix and the formation of interfaces between carbon particles, can lead to unexpected impedance behaviour (Kozai et al., 2012; Cui et al., 2014). In the literature, we can see PMMA has the higher impedance values than PU and PAC. The impedance of pure PU measured above to $10^4 \,\Omega$ at 1MHz and the impedance of Parylene C measured about 103 Ω at 0.1 MHz and see the frequency and impedance are inversely proportional (Kim & Cho, 2012; Chun et al., 2014). We can see the impedance of PMMA based doped conductive materials are about $10^6 \Omega$ range at MHz frequencies (Shamrao et al., 2019). In our study, the impedance value of samples at 1 MHz are 0.07 and 0.09 M Ω band for all measurements. These values are close to literature.

Figure 2c and 2d shows that frequency dependent variation of the resistance value of the samples before and after polarisation. The peak values of resistance at the resonance frequency are 0.7706 M Ω for the 0C and 0.8473 M Ω for the 1C before polarisation (Figure 2c), and 0.6470 M Ω for the 0C and 0.6649 M Ω for the 1C after polarisation. (Figure 2d). After polarisation, we observed that a decrease in resistance values, and when the active carbon added, the peak of resistance value increased.

The frequency response of the reactance of the samples before and after polarisation is shown in Figure 2e and 2f. As expected, the reactance changes from negative to positive with a value of 0 due to the capacitive behaviour shown in Figure 1 and the inductive behaviour shown in the resonant frequency region. In the frequency range lower than the resonant frequency, the reactance takes a negative value and its absolute value decreases and approaches 0. This is caused by the capacitive behaviour of the material (Sun et al., 2019). In the range greater than the resonance frequency values, positive reactance, i.e. inductive character is observed. This is expressed by the formula $Z''=Z_L+Z_C$ ($Z_L=\omega L$ (inductive reactance), $Z_C=1/\omega C$ (capacitive reactance)) (Z. Wang et al., 2020). The peak values of reactance before polarisation at the resonance frequency are 0.44 M Ω and -0.38 M Ω for 1C, 0.36 M Ω and - $0.40~\mathrm{M}\Omega$ for 0C, respectively. The peak values of reactance after polarisation at the resonance frequency are 0.31 M Ω and -0.35 M Ω for the 1C, 0.30 M Ω and -0.35 M Ω for the 0C, respectively.

4. Conclusion

The dielectric properties of PAC-based composite films are investigated as a function of frequency using an impedance analyzer. This study examines the effects of activated carbon doping and the polarization process on the composite films. Negative capacitance and negative dielectric permittivity are observed through dielectric resonance The analysis of the PACbased composite films reveals an inductive character at frequencies surpassing the resonance frequency. Upon polarization, the samples exhibit a notable increase in capacitance and dielectric constant, coupled with a reduction in impedance. Interestingly, the incorporation of activated carbon introduces an unexpected phenomenon: a heightened impedance peak. This observation, however, is accompanied by a moderate increase in dielectric losses. Despite this increase in losses, the overall effect of polarization remains positive, as the gains in capacitance and dielectric constant significantly outweigh the losses. Furthermore, within a specific frequency range, the composite films display remarkable properties characterized by negative capacitance, high permittivity, and low dielectric losses. This unique combination of properties holds potential for various applications in advanced electronic devices and energy storage systems. The observed negative capacitance, in particular, suggests the possibility of enhancing charge storage capabilities beyond traditional limits.

In conclusion, this study highlights the intricate relationship between polarization, activated carbon doping, and the dielectric properties of PAC-based composite films. While the addition of activated carbon introduces a trade-off between impedance and losses, the overall impact of polarization on capacitance and dielectric constant remains favorable. The discovery of negative capacitance within a specific frequency range opens up new avenues for exploring innovative materials with tailored dielectric properties. Further investigations into the underlying mechanisms responsible for these observations may lead to the development of advanced materials with enhanced performance for various technological applications. This frequency range holds potential for various metamaterial applications. However, due to the inherently low permittivity of the polymers employed, their utilization in applications demanding high permittivity may present limitations in terms of efficiency and performance.

Acknowledgment

This work was financially supported by the funds of The Scientific and Technological Research Council of Turkey (TUBITAK) (120M636) and Kastamonu University—Turkey research Grant (KUBAP-01/2022-28).

Conflict of Interest

The authors declare that they have no conflict of interest.

References

- Axelrod, E., Puzenko, A., Haruvy, Y., Reisfeld, R., & Yuri Feldman Y. (2006). Negative dielectric loss phenomenon in porous sol–gel glasses. *Journal of Non-Crystalline Solids*, 352(40-41), 4166-4173. https://doi.org/10.1016/j.jnoncrysol.2006.07.008
- Balu, S. K., Shanker, N. P., Manikandan, M., Aparnadevi, N., Mulikraj, T., Manimuthu, P., & Venkateswaran, C. (2020). Crossover to negative dielectric constant in perovskite PrMnO₃. *Physica Status Solidi A-Applications and Materials Science*, 217(17), 2000230. https://doi.org/10.1002/pssa.202000230
- Chun, W., Chou, N., Cho, S., Yang, S., & Kim, S. (2014). Evaluation of sub-micrometer parylene C films as an insulation layer using electrochemical impedance spectroscopy. *Progress in Organic Coatings*, 77(2), 537-547. https://doi.org/10.1016/j.porgcoat.2013.11.020
- Cui, W., Cheng, N., Liu, Q., Ge, C., Asiri, A. M., & Sun, X. (2014). Mo₂C nanoparticles decorated graphitic carbon sheets: Biopolymer-derived solid-state synthesis and application as an efficient electrocatalyst for hydrogen generation. *Acs Catalysis*, 4(8), 2658-2661. https://doi.org/10.1021/cs5005294
- Dong, J., Li, L., Qiu, P., Pan, Y., Niu, Y., Sun, L., Pan, Z., Liu, Y., Tan, L., Xu, X., Luo, G., & Wang, H. (2023). Scalable polyimide-organosilicate hybrid films for high-temperature capacitive energy storage. *Advanced Materials*, 35(20), 2211487. https://doi.org/10.1002/adma.202211487
- El-Nahass, M. M., Attia, A. A., Salem, G. F., Ali, H. A. M., & Ismail, M. I. (2014). Dielectric and impedance spectral characteristics of bulk ZnIn₂Se₄. *Physica B: Condensed Matter*, 434, 89-94. https://doi.org/10.1016/j.physb.2013.10.049
- Florkowski, M., Kuniewski, M., & Mikrut P. (2024). Effect of voltage harmonics on dielectric losses and dissipation factor interpretation in high-voltage insulating materials. *Electric Power Systems Research*, 226, 109973. https://doi.org/10.1016/j.epsr.2023.109973
- Hoffmann, M., Fengler, F. G. P., Herzig, M., Mittmann, T. M. B., Schroeder, U., Negrea, R. L. P., Slesazeck, S., & Mikolajick, T. (2019). Unveiling the double-well energy landscape in a ferroelectric layer. *Nature*, *565*, 464-467. https://doi.org/10.1038/s41586-018-0854-z
- Hu, Z., Liu, X., Ren, T., Saeed, H. A. M, Wang, Q., Cui, X., Huai, K., Huang, S., Xia, Y., Fu, K., Zhang, J., & Chen, Y. (2022). Research progress of low dielectric constant polymer materials. *Journal of Polymer Engineering*, 42(8), 677-687. https://doi.org/10.1515/polyeng-2021-0338
- Íñiguez, J., Zubko, P., Luk'yanchuk, I., & Cano, A. (2019). Ferroelectric negative capacitance. *Nature Reviews Materials*, *4*, 243-256. https://doi.org/10.1038/s41578-019-0089-0

- Jiang, W., Hardy, D. J., Phillips, J. C., MacKerell, A. D., Schulten, K., & Roux, B. (2010). High-performance scalable molecular dynamics simulations of a polarizable force field based on classical drude oscillators in namd. *The Journal of Physical Chemistry Letters*, 2(2), 87-92. https://doi.org/10.1021/jz101461d
- Jones, B. K., Santana, J., & McPherson, M. (1998). Negative capacitance effects in semiconductor diodes. *Solid State Communications*, 107(2), 47-50. https://doi.org/10.1016/S0038-1098(98)00162-8
- Kahouli, A., Sylvestre, A., Ortega, L., Jomni, F., Yangui, B., Maillard, M., Berge, B., Robert, J. C., & Legrand J. (2009). Structural and dielectric study of parylene C thin films. *Applied Physics Letters*, *94*(15), 152901. https://doi.org/10.1063/1.3114404
- Khan, A. I., Chatterjee, K., Wang, B., Drapcho, S., You, L., Serrao, C., Bakaul, S. R., Ramesh, R., & Salahuddin, S. (2015). Negative capacitance in a ferroelectric capacitor. *Nature Materials*, 14(2), 182-186. https://doi.org/10.1038/nmat4148
- Kim, S., & Cho, S. (2012). Parylene-C-coated indium tin oxide electrodes for the optical-and electrical-impedance characterization of cells. *Journal of Nanoscience and Nanotechnology*, 12(7), 5830-5834. https://doi.org/10.1166/jnn.2012.6363
- Kozai, T. D. Y., Langhals, N. B., Patel, P. R., Deng, X., Zhang, H., Smith, K., Lahann, J., Kotov, N. A., & Kipke, D. R. (2012). Ultrasmall implantable composite microelectrodes with bioactive surfaces for chronic neural interfaces. *Nature Materials*, 11(12), 1065-1073. https://doi.org/10.1038/nmat3468
- Kurnaz, S., Ozturk, O., Hazar, M. A., Guduloglu, U., Yilmaz, N., & Cicek, O. (2023). Flexible capacitive and piezoresistive pressure sensors based on screen-printed parylene C/polyurethane composites in low-pressure range. *Flexible and Printed Electronics*, 8(3), 035015. https://doi.org/10.1088/2058-8585/acf774
- Leng, Z., Wu, H., Tang, X., Li, Y., Xin, Y., Xie, P., Li, G., Yan, K., & Liu, C. (2020). Carbon nanotube/epoxy composites with low percolation threshold and negative dielectric constant. *Journal of Materials Science:*Materials in Electronics, 33, 26015-26024. https://doi.org/10.1007/s10854-022-09291-6
- Li, H., Ai, D., Ren, L., Yao, B., Han, Z., Shen, Z., Wang, J., Chen, L., & Wang, Q. (2019). Scalable polymer nanocomposites with record high-temperature capacitive performance enabled by rationally designed nanostructured inorganic fillers. *Advanced Materials*, 31(23), 1900875. https://doi.org/10.1002/adma.201900875
- Liu, Y., Xu, C., Ren, H., Wei, Z., & Zhang, Z. (2020). Tailorable negative permittivity in Fe/BaTiO₃ metacomposites. *Functional Materials Letters*, 13(03), 2050017. https://doi.org/10.1142/S1793604720500174

- Mokni, M., Maggioni, G., Kahouli, A., Carturan, S. M., Raniero, W., & Sylvestre, A. (2019). Nanocomposite—parylene C thin films with high dielectric constant and low losses for future organic electronic devices. *Beilstein Journal of Nanotechnology*, *10*, 428-441. https://doi.org/10.3762/bjnano.10.42
- Oughstun, K. E., & Cartwright, N. A. (2003). On the lorentz-lorenz formula and the lorentz model of dielectric dispersion. *Optics Express*, 11(13), 1541-1546. https://doi.org/10.1364/oe.11.001541
- Qu, Y., Du, Y., Fan, G., Xin, J., Liu, Y., Xie, P., You, S., Zhang, Z., Sun, K., & Fan, R. (2019). Low-temperature sintering Graphene/CaCu₃Ti₄O₁₂ nanocomposites with tunable negative permittivity. *Journal of Alloys and Compounds*, 771, 699-710. https://doi.org/10.1016/j.jallcom.2018.09.049
- Raja, V., Sharma, A. K., & Rao, V. V. R. N. (2004). Impedance spectroscopic and dielectric analysis of PMMA-CO-P₄VPNO polymer films. *Materials Letters*, 58(26), 3242-3247. https://doi.org/10.1016/j.matlet.2004.05.061
- Romano, S., Cabrini, S., Rendina, I., & Mocella, V. (2014). Guided resonance in negative index photonic crystals: A new approach. *Light: Science &Amp; Applications*, 3(1), e120. https://doi.org/10.1038/lsa.2014.1
- Sankar, S., Kanagathara, N., & Robinson Azariah, J. C. (2022). Electric modulus, dielectric relaxation mechanism and impedance properties of melaminum perchlorate monohydrate broadband dielectric spectroscopic study. *Acta Physica Polonica A*, 141(5), 500-506. https://doi.org/10.12693/APhysPolA.141.500
- Shamrao, P. V., Vithya, K., Premalatha, M., & Sundaresan, B. (2019). AC impedance study of PMMA-LiNO₃ electrolyte. *In Macromolecular Symposia*, 387(1), 1800187. https://doi.org/10.1002/masy.201800187
- Sun, K., Dong, J., Wang, Z., Wang, Z., Fan, G., Hou, Q., An, L., Dong, M., Fan, R., & Guo, Z. (2019). Tunable negative permittivity in flexible graphene/PDMS metacomposites. *The Journal of Physical Chemistry*, *123*(38), 23635-23642. https://doi.org/10.1021/acs.jpcc.9b06753
- Vandeparre, H., Watson, D., & Lacour, S. P. (2013). Extremely robust and conformable capacitive pressure sensors based on flexible polyurethane foams and stretchable metallization. *Applied Physics Letters*, 103(20), 204103. https://doi.org/10.1063/1.4832416
- Wang, D., Li, H., Li, M., Jiang, H., Xia, M., & Zhou, Z. (2013). Stretchable conductive polyurethane elastomer in situ polymerized with multi-walled carbon nanotubes.

- Journal of Materials Chemistry C, 1(15), 2744-2749. https://doi.org/10.1039/C3TC30126E
- Wang, T., Liu, S., Li, X., Wang, Q., Liu, S., Liang, X., Li, S., Liu, B., Liu, J., & Zhang, G. (2022). Wide bandgap nanocoatings for polymer dielectric with outstanding electrical strength. *Advanced Materials Interfaces*, *9*(35), 2201824. https://doi.org/10.1002/admi.202201824
- Wang, Z., Li, H., Hu, H., Fan, Y., Fan, R., Li, B., Zhang, J., Liu, H., Fan, J., Hou, H., Dang, F., Kou, Z., & Guo Z. (2020). Direct observation of stable negative capacitance in SrTiO₃@ BaTiO₃ heterostructure. *Advanced Electronic Materials*, 6(2), 1901005. https://doi.org/10.1002/aelm.201901005
- Wong, J. C., & Salahuddin S. (2018). Negative capacitance transistors. *Proceedings of the IEEE*, 107(1), 49-62. https://doi.org/10.1109/JPROC.2018.2884518
- Xie, P., Shi, Z., Feng, M., Sun, K., Liu, Y., Yan, K., Liu, C., Moussa, T. A. A., Huang, M., Meng, S., Liang, G., Hou, H., Fan, R., & Guo, Z. (2022). Recent advantages in radio-frequency negative dielectric metamaterials by designing heterogeneous composites. *Advanced Composites and Hybrid Materials*, 5, 679-695. https://doi.org/10.1007/s42114-022-00479-2
- Xu, J., Zhu, L., Fang, D., Liu, L., Wang, L., & Xu, W. (2013).
 Prediction of dielectric dissipation factors of polymers from cyclic dimer structure using multiple linear regression and support vector machine. *Colloid and Polymer Science*, 291, 551-561.
 https://doi.org/10.1007/s00396-012-2743-6
- Yan, H., Zhao, C., Wang, K., Deng, L., Ma, M., & Xua, G. (2013). Negative dielectric constant manifested by static electricity. *Applied Physics Letters*, 102, 062904. https://doi.org/10.1063/1.4792064
- Yang, P., Sun, K., Wu, Y., Wu, H., Yang, X., Wu, X., Du, H., & Fan, R. (2022). Negative permittivity behaviors derived from dielectric resonance and plasma oscillation in percolative bismuth ferrite/silver composites. *The Journal of Physical Chemistry C*, 126(30), 12889-12896. https://doi.org/10.1021/acs.jpcc.2c03543
- Yu, X., Yi, B., Liu, F., & Wang, X. (2008). Prediction of the dielectric dissipation factor tanδ of polymers with an ANN model based on the DFT calculation. *Reactive & Functional Polymers*, 68(2008), 1557-1562. https://doi.org/10.1016/j.reactfunctpolym.2008.08.009